Brain Networks Involved in Early versus Late Response Anticipation and Their Relation to Conflict Processing

Henry Lütcke[1], Holger Gevensleben[2], Björn Albrecht[2], and Jens Frahm[1]

Abstract

■ Previous electrophysiological studies have clearly identified separable neural events underlying early and late components of response anticipation. Functional neuroimaging studies, however, have so far failed to account for this separation. Here, we performed functional magnetic resonance imaging (fMRI) of an anticipation paradigm in 12 healthy adult subjects that reliably produced early and late expectancy waves in the electroencephalogram. We furthermore compared fMRI activations elicited during early and late anticipation to those associated with response conflict. Our results demonstrate the existence of distinct cortical and subcortical brain regions underlying early and late anticipation. Although late anticipatory behavior was associated with activations in dorsal ACC, frontal cortex, and thalamus, brain responses linked to the early expectancy wave were localized mainly in motor and premotor cortical areas as well as the caudate nucleus. Additionally, late anticipation was associated with increased activity in midbrain dopaminergic nuclei, very likely corresponding to the substantia nigra. Furthermore, whereas regions involved in late anticipation proved to be very similar to activations elicited by response conflict, this was not the case for early anticipation. The current study supports a distinction between early and late anticipatory processes, in line with a plethora of neurophysiological work, and for the first time describes the brain structures differentially involved in these processes. ■

INTRODUCTION

When a warning signal is presented prior to a target presentation, reaction times are faster compared to when no warning signal is presented. The underlying anticipation process is reflected in a characteristic slow cortical potential termed contingent negative variation (CNV; Walter, Cooper, Aldridge, McCallum, & Winter, 1964). Response anticipation and CNV have been investigated using two-stimulus paradigms in which the first stimulus cues a second stimulus which occurs after a predictable time interval. Short interstimulus intervals (ISIs) of ≈1 sec give rise to a sustained negativity over the entire interval (Walter et al., 1964), whereas longer ISIs of 6 to 9 sec result in a biphasic wave with early and late components (Loveless & Sanford, 1974), commonly termed initial (iCNV) and terminal (tCNV) contingent negativity (Birbaumer, Elbert, Canavan, & Rockstroh, 1990). Considerable evidence suggests that iCNV and tCNV reflect dissociable neural processes which are, at least to some degree, confounded in the monophasic wave. Whereas iCNV is strongest at bilateral frontal electrodes, tCNV has a maximum at the vertex. Furthermore, unlike iCNV, the amplitude of tCNV increases with uncertainty over the response to the imperative stimulus, compared to when the nature of the response is already determined (van Boxtel & Brunia, 1994).

Neurophysiological studies implicated an ensemble of thalamo-cortical structures in CNV generation (Birbaumer et al., 1990). Subsequently, brain regions including primary and supplementary motor areas (SMA), anterior cingulate (ACC) as well as thalamic nuclei have been implicated in CNV generation (Fan et al., 2007; Nagai et al., 2004; Ioannides et al., 1994). Nevertheless, due to the use of short ISI paradigms, previous studies did not identify distinct neural circuits associated with early and late components of the CNV. Here, we addressed this question by employing a long ISI anticipation task, which elicited dissociable early and late CNV components. Subsequently, we investigated the relation of brain regions subserving early and late components of response anticipation with activation patterns in response to conflict-eliciting stimuli in the same subjects. A recent study (Fan et al., 2007) compared neural processes underlying response anticipation as well as conflict. The authors demonstrated a set of shared and distinguishable brain regions underlying anticipation and conflict processes. Due to their use of short ISIs

[1]Biomedizinische NMR Forschungs GmbH am Max-Planck-Institut für biophysikalische Chemie, Göttingen, Germany, [2]University of Göttingen, Germany

(2.25 sec), it remains unknown how neural processes underlying different subcomponents of anticipation relate to brain regions involved in conflict resolution.

In the current study, we employed a long ISI continuous performance task (CPT; Heinrich, Gevensleben, Freisleder, Moll, & Rothenberger, 2004; van Leeuwen et al., 1998) to investigate neural correlates of early and late anticipation using functional magnetic resonance imaging (fMRI) at high spatial resolution as well as electroencephalography (EEG). Based on differential source distributions for iCNV and tCNV in previous EEG studies (Birbaumer et al., 1990), we hypothesized that early anticipation would be associated with frontal and lateral cortical regions, whereas late anticipatory processes would involve more medial areas, mainly dorsal ACC. According to previous imaging studies (Nagai et al., 2004), we expected subcortical thalamic nuclei to be involved in early and late anticipation. Furthermore, using fMRI and a Flanker task (Taylor et al., 2006; Eriksen & Eriksen, 1974), we investigated brain regions involved in conflict resolution and their relation to response anticipation. Conflict and expectancy were hypothesized to coactivate a number of brain regions, including dorsal ACC and frontal cortex (Fan et al., 2007).

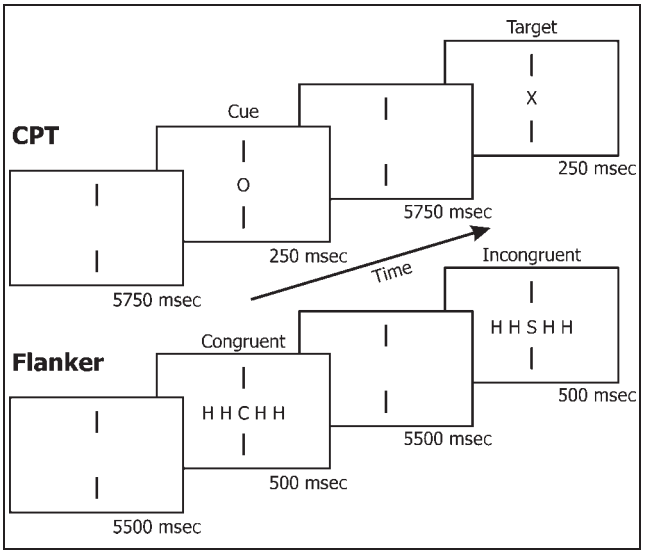

Figure 1. Schematic representation of (top) continuous performance task (CPT) and (bottom) Flanker task. In the CPT (top), subjects were instructed to respond with a button press if the cue letter (O) was followed by a target letter (X) but not if it was followed by a distracter (H, not shown). For the Flanker task (bottom), subjects were asked to respond with a right-hand button press if the odd-one-out letter was a "C" or "H", whereas a left-hand response was required for "K" or "S". Flanking (distracter) stimuli were also chosen from this same set of four letters, so that they could be associated with the same hand response as the target letter (congruent trial) or the opposite hand response (incongruent trial). Note that targets were only presented in one of the three central positions.

METHODS

Subjects

Twelve right-handed volunteers (3 men and 9 women; mean age = 28 ± 6 years) participated in both CPT and Flanker experimental sessions (carried out on separate days). CPT data from one subject were discarded due to excessive head motion (mean displacement of more than 1 mm in any direction). During each experiment, subjects performed four or five repetitions of the task, leaving us with a total of 53 CPT and 47 Flanker runs for analysis. For logistic reasons, we generally performed the CPT experiments prior to the Flanker session. This order was reversed for three subjects. All participants were informed about the purpose of the study as well as possible risks associated with magnetic resonance imaging (MRI). Written consent was obtained prior to each experimental session. Participants earned 10 Euros per hour plus a bonus depending on their performance. All experimental procedures conformed fully to institutional guidelines.

CPT Task

We employed a cued version of the CPT that has been shown to reliably elicit a CNV in previous EEG studies (Heinrich et al., 2004). Subjects were presented with the letters O, X, or H (ISI = 5750 msec) and were instructed to press the response button with their right thumb or index finger only for an X (target), if it was preceded by an O (see Figure 1). Therefore, the O acted as a cue to orient subjects' attention to a possible target. However, only in 50% of the cases did an X actually follow the cue, whereas an H (distracter) was presented in the remaining trials. Crucially, the distracter could also be presented in place of a cue, signifying to the subject that any subsequent letter is irrelevant, as no response would be required on the next trial. Because tCNV amplitude increases with uncertainty about the response to the cued stimulus (van Boxtel & Brunia, 1994), we reasoned that cues would produce substantially stronger response anticipation compared to distracters (noncues). The crucial contrast reflecting late anticipatory processes was therefore obtained by a comparison of brain activity during the 4- to 6-sec time interval following a cue versus a noncue. Conversely, early anticipation was indexed by the same contrast, which was, however, focused on the 0- to 2-sec time window following a cue. Cues elicited stronger early waves in the EEG compared to distracters (see below), which may reflect enhanced preparatory activity for upcoming responses to S2 (Bender, Resch, Weisbrod, & Oelkers-Ax, 2004). Over the whole experiment, the probability of an O–X pair (cue–target) as well as O–H (cue–distracter) was 20% each. Additionally, there was a 10% probability of an uncued X (nontarget) or H being shown. In order to encourage fast responses, letters were shown very briefly (250 msec). Correct responses to targets had to occur within 1000 msec of stimulus presentation. All stimuli were presented in

black color on a white background. Two black vertical bars were continuously presented above and below the stimulus location in order to direct subjects' attention to the center of the screen.

Flanker Task

A letter version of the Eriksen flanker task was used in the present study (Taylor et al., 2006; Eriksen & Eriksen, 1974). Stimuli consisted of a string of four distracter and one target letter, presented in the center of the screen. Subjects had to identify the odd letter and make a response: right-hand button press for ''C'' or ''H'' and left-hand button press for ''K'' or ''S'' (see Figure 1). Crucially, the distracters consisted of letters from this same set of four letters. On congruent trials, both targets and distracters indicated the same response, whereas on incongruent trials distracters were associated with the opposite hand as the target. Target letters were allowed to occur in one of the three central positions of the five-letter string. Pseudorandom stimulus sequences were generated such that the same number of congruent and incongruent as well as left- and right-hand trials was presented during a run. Furthermore, the occurrence of more than three consecutive congruent or incongruent and left- or right-hand trials was not allowed. Stimuli were presented for 500 msec and appeared in white color on a black background. Subjects were required to respond within 1500 msec of stimulus presentation. As in the CPT, two vertical bars were continuously presented to focus subjects' attention. Congruent and incongruent trials were modeled as a 1-sec boxcar function following the onset of a respective trial.

In both the CPT and Flanker task, a total of 80 stimuli were presented with a stimulus onset asynchrony of 6 sec using a computer running Presentation (Neurobehavioral Systems, Albany, CA) and interfaced with a dedicated projection setup (Schäfter & Kirchhoff, Hamburg, Germany) or MRI-compatible liquid crystal display goggles (Resonance Technology, Northridge, CA). Corrective lenses were applied if necessary. Button presses were recorded with custom-built MRI-compatible response boxes. For each run, the sequence of stimuli to be presented was randomly selected from a list of four possible sequences, which had been previously generated to fulfill the aforementioned criteria. The duration of a single experimental run was about 8 min.

Magnetic Resonance Imaging

All studies were conducted at 3 T (Siemens Tim Trio, Erlangen, Germany) using a 12-channel receive-only head coil in combination with the whole-body coil for radiofrequency pulse transmission. For each subject, we acquired a T1-weighted MRI dataset using a 3-D MP-RAGE sequence at $1.3 \times 1 \times 1.3$ mm^3 resolution for anatomic referencing (interpolated to $1 \times 1 \times 1.3$ mm^3). For fMRI, we employed a single-shot, gradient-echo EPI sequence (TR/TE = 2000/36 msec, flip angle 70°, 244 volumes per run) with a voxel size of $2 \times 2 \times 4$ mm^3 (84×96 acquisition matrix, 192 mm FOV, 7/8 partial Fourier phase encoding, bandwidth 1336 Hz/pixel, echo spacing 0.81 msec). We acquired 22 slices without gap, positioned in the transverse-to-coronal plane approximately parallel to the corpus callosum and covering the whole cerebrum. At the end of each session, one EPI volume was acquired with the same specifications as the functional series but covering the whole brain (36 slices) in order to facilitate registration of fMRI data to the anatomical scan. Proton-density weighted MRI was performed in a subset of subjects to identify the precise anatomical location of dopaminergic nuclei in the midbrain (fast spin-echo sequence, 9 echoes, resolution $0.8 \times 0.8 \times 1.9$ mm^3, 39 slices without gap, flip angle 149°, TR/TE = 6000/16 msec, bandwidth 98 Hz/pixel, echo spacing 15.6 msec). Dopaminergic nuclei, especially the substantia nigra (SN), present as hyperintensities in this acquisition mode (Oikawa, Sasaki, Tamakawa, Ehara, & Tohyama, 2002).

MRI Data Analysis

For both tasks (CPT and Flanker), only correct trials were included in the analysis. Evaluation of fMRI data was performed using tools from the FMRIB Software library (FSL; www.fmrib.ox.ac.uk) and MATLAB (The MathWorks, Natick, MA). Statistical analysis was performed in SPSS (SPSS, Chicago, IL). Scans were corrected for subject motion both in *k*-space (Siemens, Erlangen, Germany) as well as by image-based registration (Jenkinson, Bannister, Brady, & Smith, 2002). Data were smoothed using a Gaussian kernel of 5 mm full width at half maximum. Nonbrain tissue was removed (Smith, 2002) and all volumes were intensity-normalized by the same factor and temporally high-pass filtered (Gaussian-weighted least-squares straight line fitting, with high-pass filter cutoff at 30 sec).

Boxcar models (see above) were convolved with a Gamma function to take into account temporal properties of the hemodynamic response (HR). Model fit was determined by statistical time-series analysis in the framework of the general linear model (GLM) and with local autocorrelation correction (Woolrich, Ripley, Brady, & Smith, 2001). For CPT experiments, contrasts between cue and noncue trials were calculated as an index of response anticipation (iCNV and tCNV), as outlined above. Correspondingly, the contrast of incongruent and congruent trials in the Flanker task presented a measure of response conflict.

Functional images were spatially normalized to the MNI152 template brain as well as to their respective anatomical scan. To summarize results across all subjects, mixed-effects group analysis was performed (Woolrich, Behrens, Beckmann, Jenkinson, & Smith, 2004; Beckmann, Jenkinson, & Smith, 2003). Unless otherwise indicated, significant activations based on *Z* statistic (Gaussianized T/F)

images were obtained by cluster thresholding (Worsley, Evans, Marrett, & Neelin, 1992) with an initial threshold of $Z > 3.1$, which was followed by a corrected cluster threshold of $p = .05$.

In our CPT paradigm, processes underlying the generation of iCNV and tCNV are separated by approximately 2 to 3 sec, a relatively short time frame in comparison to the HR latency. Given the substantial variability in the shape of the HR function (Aguirre, Zarahn, & D'Esposito, 1998), model-based fMRI analysis, as outlined above, may not be suitable for distinguishing neural correlates of early and late anticipation. We verified the validity of the CPT GLM by performing a model-free tensorial independent component analysis (TICA; Beckmann & Smith, 2005), as implemented in FSL. To this end, repetitions with the same pseudorandom stimulus sequence were averaged across subjects and decomposed into sets of vectors which describe signal variation across the temporal domain (time courses), the subject domain, and across the spatial domain (maps) by optimizing for non-Gaussian spatial source distributions using a fixed-point iteration technique (Hyvärinen, 1999). Estimated component maps were divided by the standard deviation of the residual noise and thresholded by fitting a mixture model to the histogram of intensity values (Beckmann & Smith, 2004). Subsequently, we examined the correspondence of identified components with the previously determined models of iCNV and tCNV. The higher error rate on the Flanker task (see below) precludes application of TICA to this test.

For quantitative analysis, regions of interest (ROI) were defined in relevant brain areas using probabilistic atlases integrated into FSL version 4 (for details, see www.fmrib.ox.ac.uk/fsl/fslview/atlas-descriptions.html). Definition of primary and premotor cortices was guided by the Jülich histological atlas (Eickhoff et al., 2005; Geyer et al., 1996). The superior frontal gyrus (SFG), supplementary motor area (SMA), and ACC were defined based on the Harvard–Oxford cortical structural atlas, as implemented in FSL. Equally, subcortical structures (thalamus, caudate nucleus, and putamen) were defined in accordance with the Harvard–Oxford subcortical structural atlas. Finally, a midbrain ROI in the SN was determined according to the Talairach atlas after the application of a correcting affine transform to register it into MNI152 space (Lancaster et al., 2007). Anatomical identification of activated brain regions in standard space was also facilitated by the aforementioned atlas tools.

For each ROI, the mean activation levels for conflict, iCNV and tCNV contrasts were extracted. As the number of subjects was comparatively low in the current study, concerns about nonnormal distribution of mean activation levels led us to adopt nonparametric techniques for statistical comparison. Means from each ROI were subjected to a Friedman's (1937) test and, pending a significant overall group difference ($p < .05$), subsequent post hoc comparisons were performed using Wilcoxon's signed rank procedure (Wilcoxon, 1945). All p values were determined by Monte Carlo simulation based on 10,000 sampled tables and randomized starting seeds.

EEG Validation of the CPT

Validity of the continuous performance test was evaluated in a separate sample of 27 healthy adults (4 men), aged 19 to 37 years (mean = 24.7 years) that performed the same task as used for fMRI while an EEG was recorded. This was done to ensure maximal comparability to existing work (Bender et al., 2004; Birbaumer et al., 1990) and to avoid side effects of practice. Note that in the EEG study, stimuli were presented in the center of a 17-inch CRT monitor with 800 × 600 points resolution against a light gray background at a viewing angle of 1.5° vertically and 1.0° horizontally.

The EEG was recorded with Ag/AgCl electrodes and Abralyt 2000 electrode cream from 23 sites according to an extended 10–20 system using a BrainAmp amplifier. An electrooculogram (EOG) was recorded from two electrodes placed above and below the right eye and at the outer canthi. Impedances were kept below 10 kΩ. EEG and EOG were recorded simultaneously to FCz as recording reference at a sampling rate of 500 Hz with low and high cutoff filters set to 0.016 and 100 Hz, respectively, and a 50-Hz notch filter. The ground electrode was placed at the forehead.

Further analyses were computed with the Vision Analyzer 1.05 software. After downsampling to 256 Hz, the EEG was re-referenced to the average and filtered off-line with 0.05–30 Hz, 24 dB/Oct Butterworth filters. Ocular artifacts were corrected using the method of Gratton and Coles without raw average subtraction (Gratton, Coles, & Donchin, 1983). Trials with performance errors, amplifier saturation, or artifacts exceeding ±100 μV amplitude at any EEG channel were rejected; stimulus-locked segments (−200 to +6300 msec around stimulus onset) were subsequently checked and averaged for cues and uncued distracters. All averages contained at least 20 sweeps. To avoid distortion of ERP topography, no baseline subtraction was applied.

RESULTS

Task Validation: CPT

Inspection of the grand-average waveforms revealed that iCNV was maximal at fronto-central sites (FCz) between 500 and 1500 msec, whereas tCNV had a more central distribution (Cz) between 4000 and 6000 msec after cue onset (see Figure 2). For the given time frames and electrodes, both mean amplitudes of iCNV and tCNV following cues could be differentiated from the respective amplitudes following uncued distracters [$t(26) = 4.12$, $p < .01$ and $t(26) = 6.03$, $p < .01$, respectively].

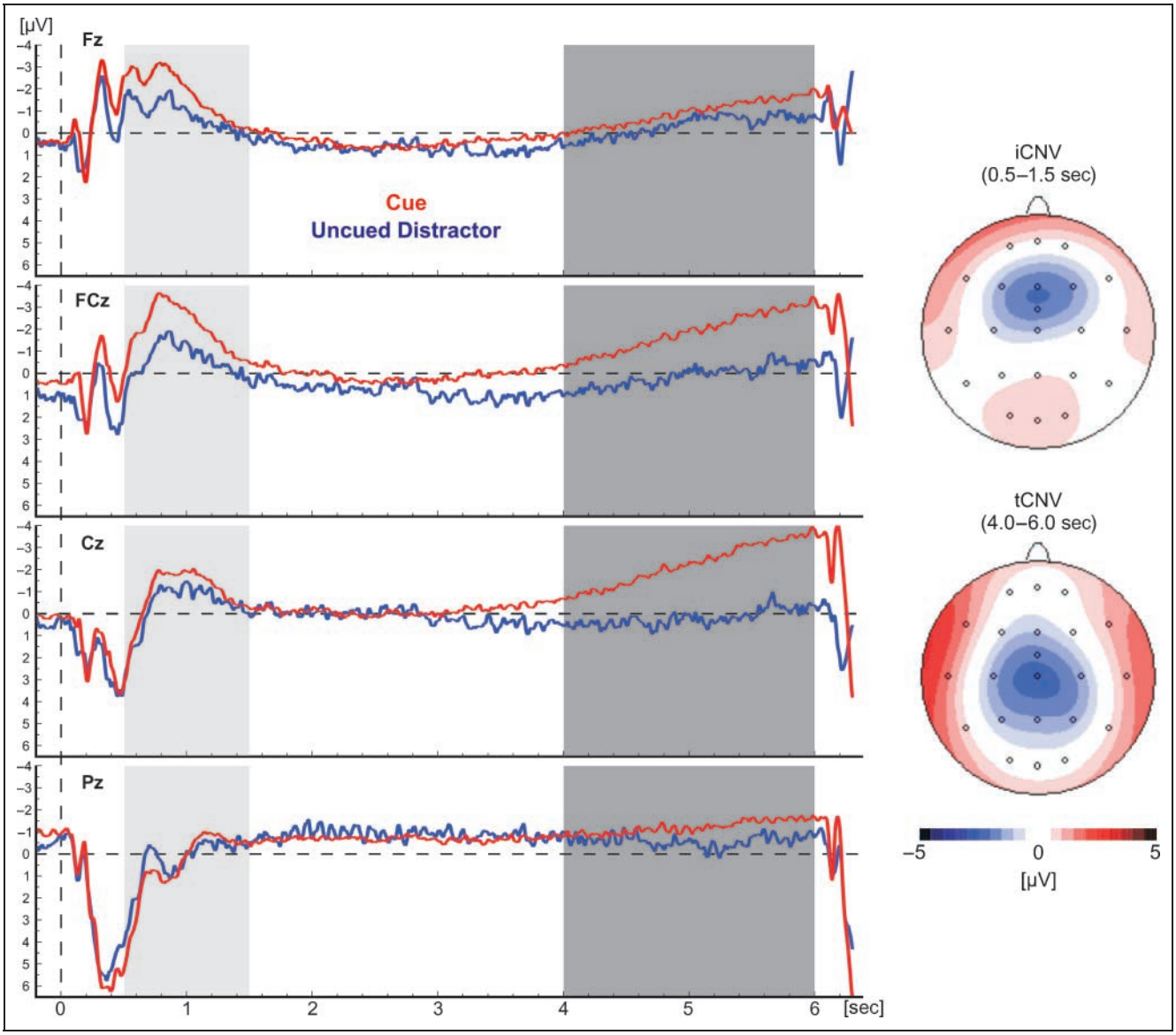

Figure 2. Group-averaged, stimulus-locked event-related potentials (left) to cues (red) and uncued distracters (blue) reveal an iCNV, which was maximal at fronto-central sites (FCz) between 0.5 and 1.5 sec (light shading) as well as a tCNV, which was strongest at the vertex (Cz) between 4 and 6 sec (dark shading). Spline-interpolated maps (right) of mean amplitudes for iCNV (0.5 to 1.5 sec) and tCNV (4 to 6 sec) following cues illustrate the differential source distribution of early and late CNV components along the anterior–posterior axis.

Task Validation: Flanker

Responses were more accurate as well as faster on congruent compared to incongruent trials. A 2 × 4 repeated measures analysis of variance (ANOVA) with congruency (congruent–incongruent) and practice (runs 1–4) as factors revealed that subjects responded significantly faster on congruent compared to incongruent trials [median reaction times = 669 and 735 msec, respectively; $F(1, 10) = 79.98$, $p < .001$]. This positive compatibility effect proved to be extremely robust, being present in every run and every volunteer. Reaction times did not change with increased practice on the task and there was no evidence for an interaction between the two factors [both $F(3, 30) < 1$]. An equivalent ANOVA was performed for accuracy, also revealing the positive compatibility effect with subjects responding more accurately on congruent compared to incongruent trials [median accuracy 98% and 91%, respectively; $F(1, 10) = 21.73$, $p = .001$]. Subjects' accuracy improved slightly over the four runs [$F(3, 30) = 2.68$, $p = .065$], which was mainly due to improvements on incongruent trials, as shown by a significant interaction [$F(3, 30) = 2.96$, $p = .048$].

Neuroimaging: Early versus Late Components of Anticipation

A standard GLM revealed distinct, nonoverlapping brain regions associated with early and late components of

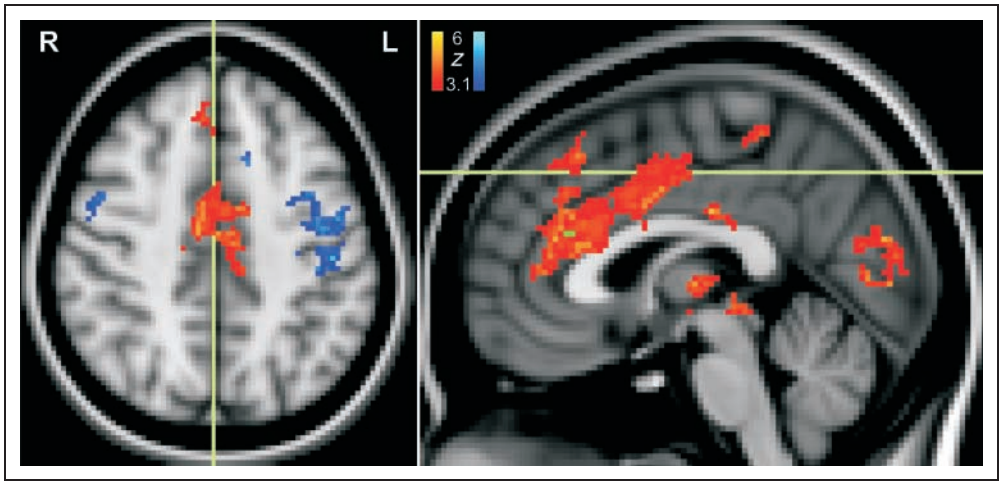

Figure 3. Brain activations during early (blue) and late (red) response anticipation as defined by iCNV and tCNV (axial and mid-sagittal section). The crucial contrast reflecting anticipatory processes was obtained by a comparison of activity following cues and noncues. Whereas tCNV is associated with more medial responses, especially in dorsal parts of ACC, iCNV evokes stronger activations in motor regions, including premotor cortex bilaterally and left motor cortex. Overlap = green.

response anticipation. As shown in Figure 3, within medial frontal cortex, dorsal ACC was significantly activated during late anticipation only (see also Table 1). Brain activation related to the iCNV, on the other hand, was located mainly in motor regions, including left primary sensorimotor cortex as well as left and right premotor cortices (see Figure 3 and Table 1).

These results were independently verified using a model-free approach based on a tensorial extension of the independent component analysis for group fMRI data (see Methods). We identified separate spatio-temporal components which were associated significantly with early and late anticipation processes. Component 4, which accounted for 3.6% of the explained variance, presented MFC activation mainly in dorsal ACC (see Figure 4) and was associated significantly with the tCNV ($Z = 4.90, p < .001$) but not the iCNV ($Z = -0.78, p = .78$) predictor of the GLM. Contrarily, Component 11 (2.9% explained variance) identified significant brain activation in left as well as right premotor cortices and was associated with iCNV ($Z = 1.76, p = .04$) but not tCNV ($Z = -1.89, p = .97$).

Outside MFC, early and late anticipation processes were associated with partially overlapping activation in cortical and subcortical brain regions (see Table 1). Notably, increased brain activation related exclusively to iCNV was observed in the caudate nucleus. Furthermore, responses in the putamen and the pallidum remained elevated throughout the anticipation interval, as evidenced by significant activation for iCNV and tCNV contrasts (see Figure 5A). Finally, we detected an extensive set of brain regions putatively underlying generation of the tCNV, including the putamen and thalamus bilaterally, as well as insular cortex and right fronto-polar cortex (FPC; see Figure 5 and Table 1). Surprisingly, tCNV generation was additionally associated with clearly enhanced activity in a midbrain region most likely corresponding to the dopaminergic nuclei of the SN (see Figure 6).

Table 1. Brain Activations during Early (iCNV) and Late (tCNV) Response Anticipation: Center-of-Gravity (COG) Coordinates (in MNI Space), Maximum *Z*-Score, and Size of Significantly Activated Clusters

Contrast	*Brain Region*	*COG Coordinates (x, y, z)*	*Z-Score*	*Volume (cm^3)*
iCNV	Left motor cortex	−44, −20, 48	5.03	5.76
	Right premotor cortex	50, 2, 38	4.48	0.71
	SMA	−10, 6, 52	4.35	0.37
	Left caudate	−16, 10, 10	4.83	2.42
	Right caudate	14, 18, 0	4.19	0.42
	Left putamen	−20, 6, 2	4.93	1.90
	Right putamen	22, 12, 0	5.07	1.57
tCNV	ACC	2, 18, 30	5.15	14.82
	Right FPC	34, 54, 18	4.78	0.85
	Left insula	−38, 8, 2	5.07	6.91
	Right insula	40, 10, 4	5.41	5.45
	Left thalamus	−8, −14, 4	5.91	5.10
	Right thalamus	12, −16, 4	5.39	6.85
	Left putamen	−24, 0, 0	5.21	9.78
	Right putamen	26, −2, 0	5.29	7.85
	Left/right SN	−6/12, −20, −14	3.18/3.62	0.49/0.95

ACC = anterior cingulate cortex; FPC = fronto-polar cortex; SMA = supplementary motor area; SN = substantia nigra.

Neuroimaging: Response Conflict and Anticipation

Brain activations due to response conflict were identified by contrasting incongruent with congruent Flanker trials. This analysis revealed a large cluster in MFC, extending from dorsal ACC into the posterior part of the SFG, a region corresponding to the pre-SMA (Rushworth, Walton, Kennerley, & Bannerman, 2004). As shown in

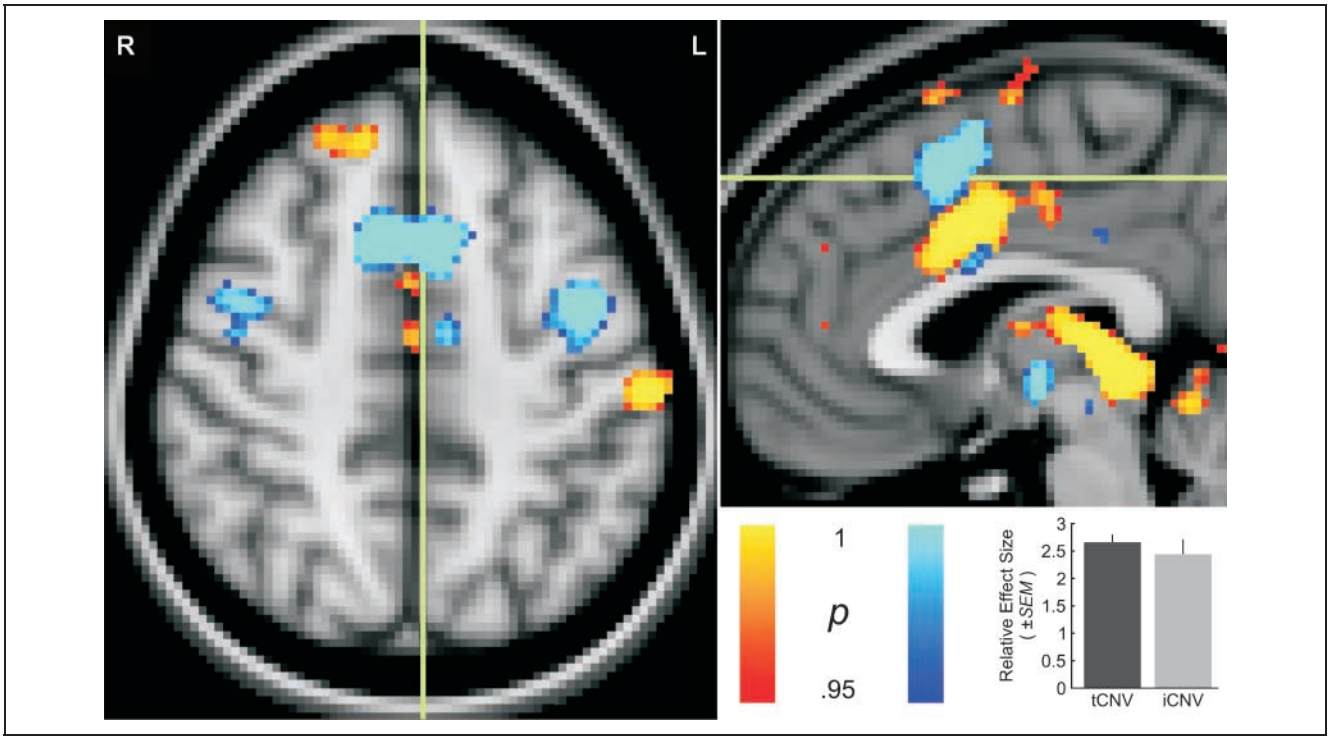

Figure 4. Brain activations obtained for a tensorial-independent component analysis (TICA; see Methods) confirm the model-based analysis by resulting in different activation patterns for early (blue–green) and late (red–yellow) response anticipation (axial and left-hemispheric sagittal section). In agreement with Figure 3, late anticipation revealed ACC activation, whereas early anticipation evoked activity in right and left lateral premotor cortices and medial supplementary motor area. Inset: Effect sizes for the identified components proved to be very consistent in the subject population.

Figure 7A, conflict-related brain responses in dorsal ACC overlapped substantially with tCNV activation. The network of brain regions shared between conflict and late anticipatory processing furthermore included right FPC, anterior insular cortex, as well as parts of the thalamus (see Figure 5B and Table 2). Contrarily, brain responses due to early anticipation failed to show any pronounced overlap with conflict-related activations (see Figure 7B).

ROIs were defined and analyzed as outlined above (see Methods). Results from cortical ROIs are summarized in Figure 8 and largely agree with the image-based analysis. Most notably, ACC responded significantly

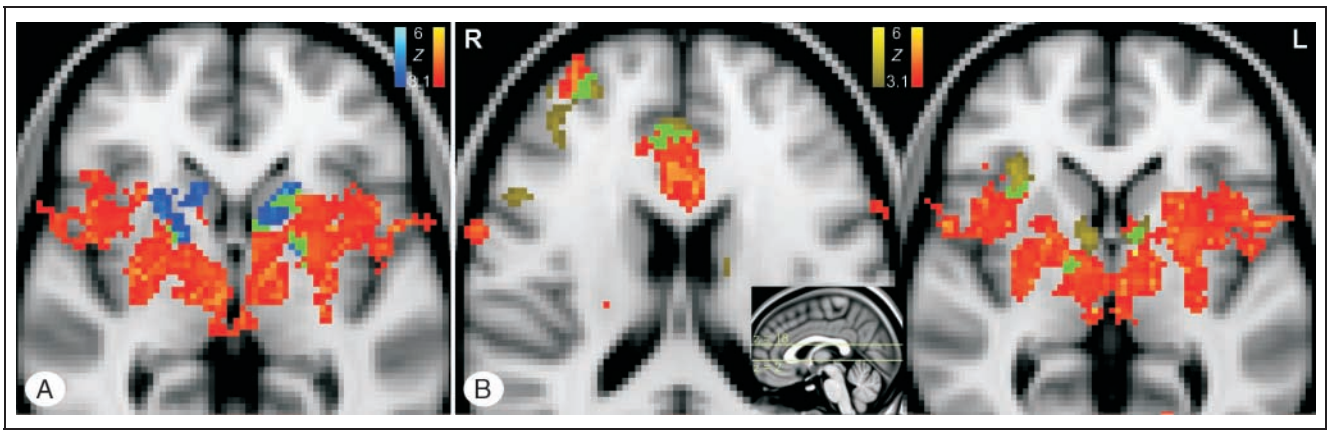

Figure 5. (A) Brain activations during early (blue) and late (red) anticipation (axial section at $z = 0$ mm). The caudate nucleus activated mainly for iCNV-related processing (especially in the right hemisphere). Other subcortical nuclei, including the putamen bilaterally, were activated during the entire anticipation interval (green). (B) Brain activations during late anticipation (red) and conflict (yellow) outside medial frontal cortex. (Left) Right FPC activated significantly for both anticipation and conflict, as shown by the substantial overlap (green). Note also the activation for both processes in ACC (see also Figure 7). (Right) A large subcortical network, including the thalamus and the putamen, was activated for late anticipation. Note also the strong activation in insular cortex, bilaterally. Conflict-related activations were observed in anterior insular cortex and anterior thalamic nuclei.

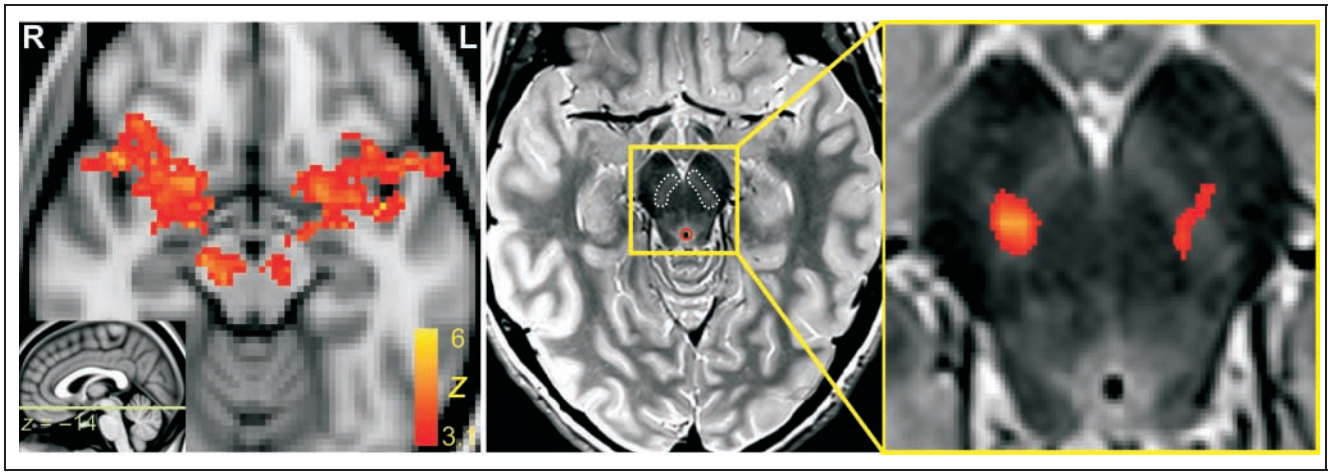

Figure 6. Brain activations during late anticipation (red) in the SN (left) for the group of 12 subjects in MNI152 standard space. (Middle) Proton-density weighted MRI identifies the midbrain dopaminergic nuclei as hyperintensities (dotted white circles). As anatomical reference, the cerebral aqueduct has been highlighted in red. (Right) The overlap of functional and anatomical images in a single subject demonstrates the activations to lie exactly within the SN.

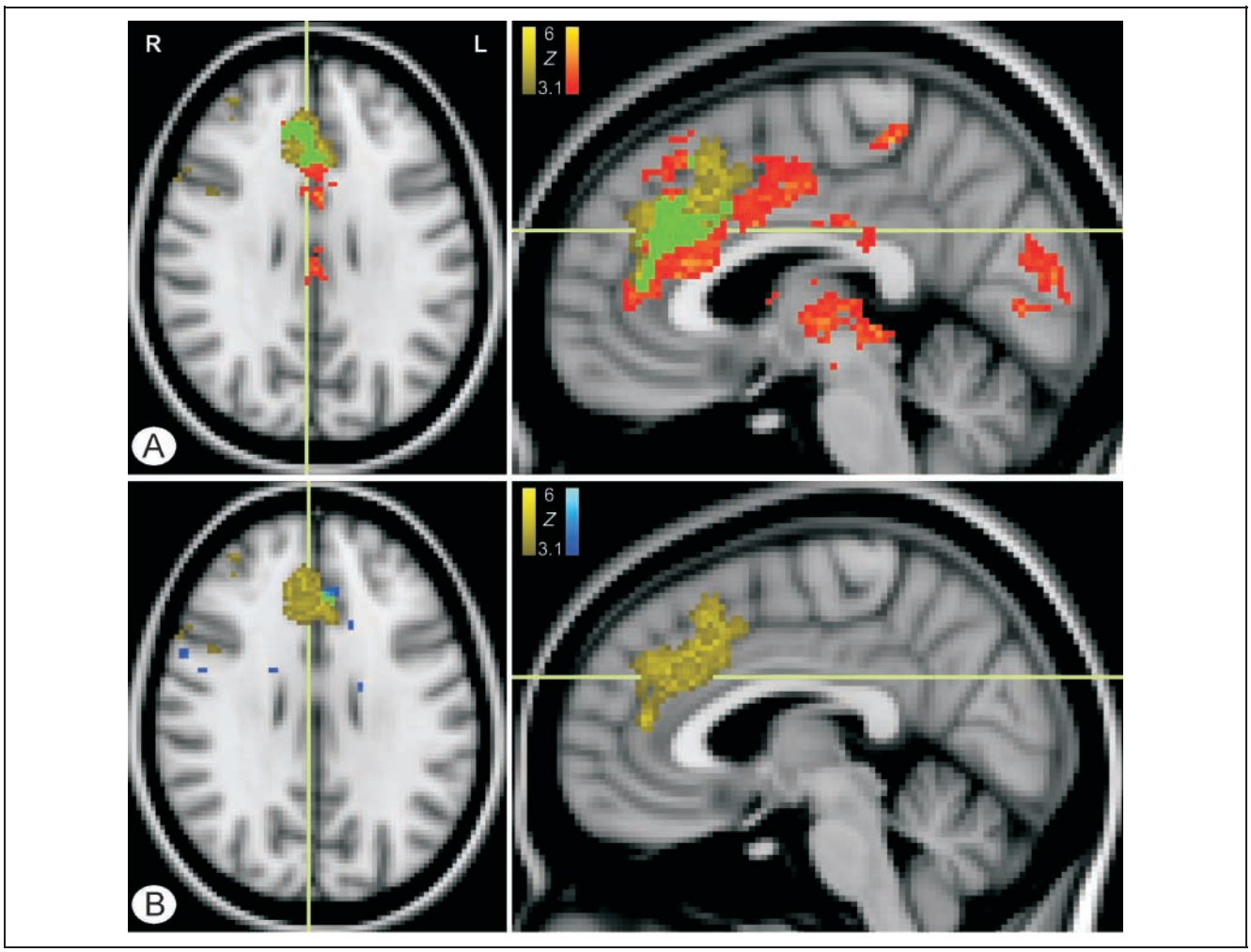

Figure 7. (A) Brain activations during late response anticipation (red) in comparison to conflict (yellow, axial and sagittal section). Note the substantial overlap (green) between both processes especially in the dorsal part of ACC. Along the SFG, on the other hand, conflict-related activation is located more posteriorly in a region corresponding to the presupplementary motor area (pre-SMA) while activations due to anticipation are observed in the anterior SFG. (B) Early response anticipation (blue) is associated with activation in different brain regions, compared to conflict processing (yellow, axial and sagittal section), as shown by the limited overlap (green).

Table 2. Brain Activations during Conflict Processing (Incongruent > Congruent): Center-of-Gravity (COG) Coordinates (in MNI Space), Maximum *Z*-Score, and Size of Significantly Activated Clusters

Contrast	*Brain Region*	*COG Coordinates (x, y, z)*	*Z-Score*	*Volume (mm^3)*
Conflict	MFC	2, 26, 36	5.18	13.43
	Right FPC	36, 46, 18	4.04	1.26
	Left IPS	−28, −62, 40	4.35	0.90
	Right IFG	50, 16, 22	4.23	0.78
	Right anterior insula	34, 24, −6	4.49	1.77
	Left anterior thalamus	−10, 2, 8	4.01	1.02
	Right anterior thalamus	12, 0, 4	4.14	1.6

MFC = medial frontal cortex; FPC = fronto-polar cortex; IPS = intraparietal sulcus; IFG = inferior frontal gyrus.

stronger during late anticipation, compared to either iCNV or conflict ($Z = 2.67$, $p = .002$ and $Z = 2.93$, $p = .001$, respectively). Although iCNV and conflict responses in ACC did not differ significantly from each other ($Z = 0.36$, $p = .4$), note that conflict elicited a small, yet significant response in ACC (one-sample Wilcoxon signed rank test; $Z = 2.67$, $p = .008$), whereas iCNV failed to do so ($Z = 0.8$, $p = .4$), in line with the qualitative image analysis. Early anticipatory processing did, however, increase the activation level in left primary somatomotor cortex ($Z = 2.58$, $p = .003$ and $Z = 2.93$, $p < .001$) as well as premotor cortices bilaterally ($Z = 1.33$, $p = .1$ and $Z = 2.93$, $p = .001$), compared to both tCNV and conflict (see also Figure 8). Finally, signal intensity in the SFG was significantly elevated for tCNV and conflict ($Z = 1.96$, $p = .02$ and $Z = 1.42$, $p = .08$), compared to iCNV.

An equivalent quantitative ROI analysis in subcortical brain structures (see Figure 8) revealed significantly enhanced activation for late anticipation, compared to both iCNV and conflict in the thalamus ($Z = 2.67$, $p = .002$ and $Z = 2.85$, $p = .001$) as well as the SN ($Z = 1.51$, $p = .08$ and $Z = 2.31$, $p = .01$). Across subjects, tCNV-related activation levels in the SN correlated strongly with brain responses in ACC ($r = .8$, $p = .007$) and FPC ($r = .7$, $p = .02$). On the other hand, thalamic activation related to late anticipation correlated with FPC ($r = .81$, $p = .003$) but not ACC ($r = .36$, $p = .27$) activation. Similar to ACC, the thalamus responded significantly to conflict ($Z = 2.20$, $p = .03$) but not to iCNV ($Z = 1.16$, $p = .25$). In line with the image-based evaluation, the caudate nucleus in the right hemisphere activated significantly stronger during early anticipatory processing compared to both tCNV ($Z = 2.05$, $p = .02$) and conflict ($Z = 1.87$, $p = .03$). Accordingly, the left caudate nucleus was significantly stronger activated during iCNV compared to conflict ($Z = 2.40$, $p = .006$), whereas the comparison of iCNV and tCNV activation levels just failed to reach statistical significance ($Z = 1.33$, $p = .1$; see also Figure 8).

DISCUSSION

In this study, we measured neural processes underlying early and late components of response anticipation and related them to brain responses evoked by cognitive conflict. We determined distinct brain regions underlying the generation of the iCNV, an electrophysiological index of early anticipatory processes, and tCNV, which is thought to reflect late anticipation. Furthermore, activations elicited by response conflict and late anticipation proved to be similar, whereas early preparatory activity implicated a distinct set of brain regions.

Neural Basis of Response Anticipation

Using a CPT paradigm with a long ISI, we reliably elicited a biphasic CNV with clear initial (0.5–1.5 sec) and terminal (4–6 sec) components, as has been shown in previous studies (Birbaumer et al., 1990; Rohrbaugh, Syndulko, & Lindsley, 1976; Loveless & Sanford, 1974; Connor & Lang, 1969). fMRI allowed us to investigate the neural processes underlying generation of iCNV and tCNV. Interestingly, distinct brain regions were associated with generation of the early and late waves of the CNV. While iCNV-related activation was mainly observed in lateral motor and premotor areas, including left primary motor cortex, which is involved in right-hand button presses, tCNV seemed to be generated by more medial brain responses, most notably including ACC. In fact, these cortical activation patterns correspond well to previous EEG research which has shown a frontal predominance for iCNV, probably corresponding to activation of premotor areas, and a more centro-medial predominance underlying tCNV generation, probably corresponding to dorsal ACC (Gomez, Marco, & Grau, 2003).

Previous functional imaging studies of response anticipation (Fan et al., 2007; Nagai et al., 2004) have identified a large subcortical network, including thalamic as well as basal nuclei, associated with CNV generation. Here we show that the majority of reported regions, especially in the thalamus, are in fact associated with the late component of response expectancy. Early wave generation, on the other hand, was found to be linked to activation in a separate subcortical region, the caudate nucleus. Interestingly, several recent functional imaging studies have shown that among basal ganglia nuclei, the caudate nucleus is more involved in executive and planning processes (e.g., Cools, Clark, & Robbins, 2004; Lewis, Dove, Robbins, Barker, & Owen, 2004),

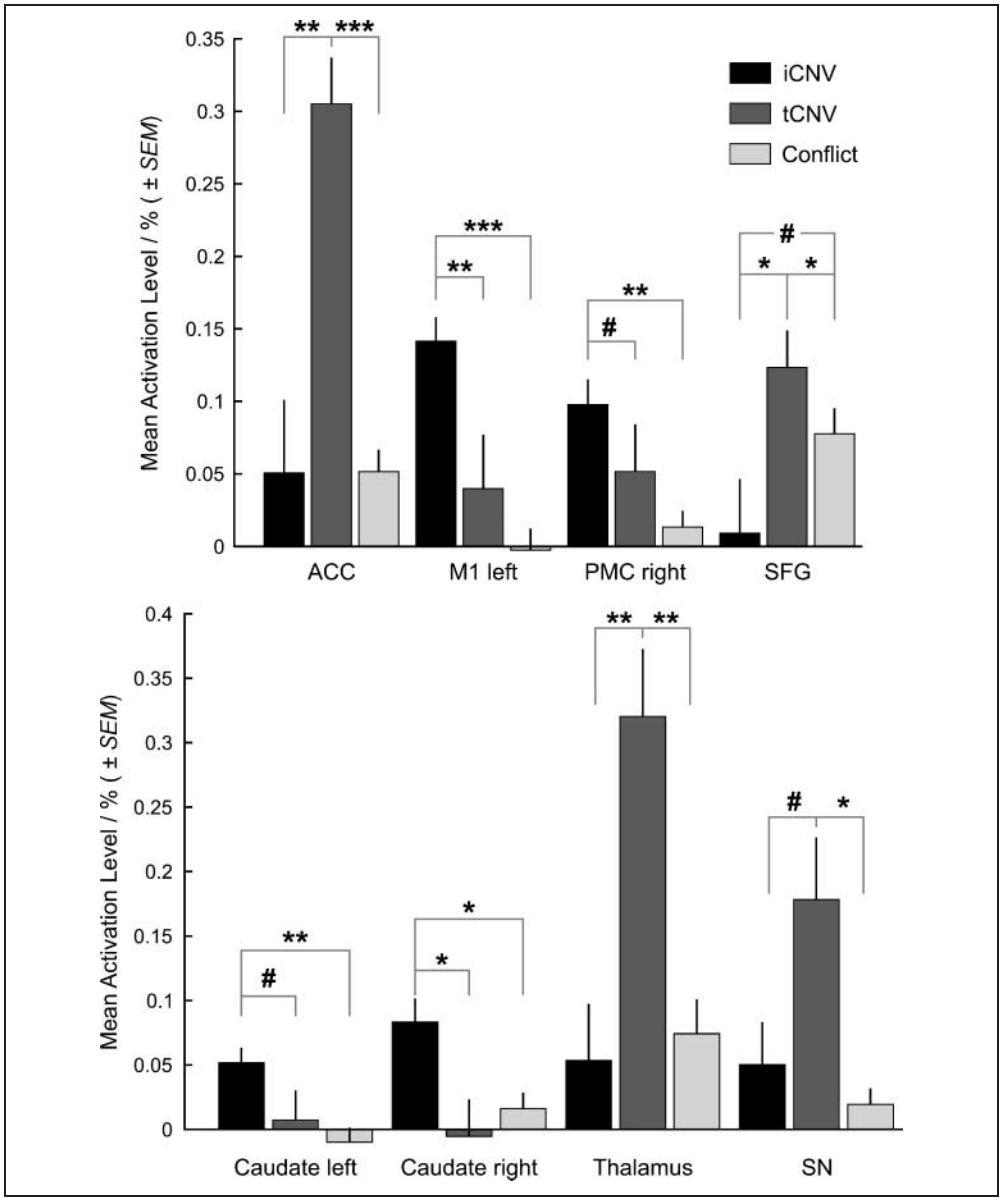

Figure 8. Normalized mean activation levels (FSL contrast of parameter estimates) provide a means of quantifying a regions modulation by early (iCNV) and late (tCNV) response anticipation as well as conflict. Results are shown for (top) cortical and (bottom) subcortical ROIs. For a definition of respective areas see text. All p values were determined using nonparametric statistics, as described above (see Methods). ACC = anterior cingulate cortex; M1 = primary somatomotor cortex; SFG = superior frontal gyrus; SN = substantia nigra. $^{***}p < .001$; $^{**}p < .01$; $^{*}p < .05$; $^{\#}p < .1$.

whereas the putamen and other structures have commonly been associated with motor-related activation.

Finally, we here provide evidence, for the first time to our knowledge, of a direct involvement of the SN in the generation of the late wave of the CNV. The absence of midbrain activation in previous fMRI studies of response anticipation may be due to a number of reasons. It is conceivable that short ISI paradigms, which may present a superposition of early and late waves (see below), do not elicit substantial SN activity. It seems more likely, however, due to the small size of the nuclei and their location deep in the brain, that signal enhancement in the SN may be particularly difficult to detect. Here we benefited from the enhanced contrast-to-noise ratio offered by multiple receiver coils as well as a relatively high spatial resolution, which may boost BOLD signal detection in small brain structures due to reduced partial volume effects. SN activation during response anticipation is in line with previous EEG studies demonstrating reduced CNV amplitude in patients suffering from Parkinson's disease (Ikeda et al., 1997; Pulvermüller et al., 1996), which is a neurological disorder characterized by degeneration of dopaminergic neurons in the substantia nigra pars compacta. Parkinson's disease seems to impair tCNV selectively, but not other slow cortical potentials, such as iCNV or the Bereitschaftspotential (Ikeda et al., 1997). Furthermore, the CNV amplitude difference between patients and controls was shown to be most pronounced at the cortical midline (Praamstra, Meyer, Cools, Horstink, & Stegeman, 1996), in line with the significant correlation between SN and ACC activation observed in our study. Interestingly, recent evidence suggests that neurophysiological impairments in Parkinson's disease may be associated with behavioral

deficits in anticipation paradigms, as shown by reduced temporal preparation (Praamstra & Pope, 2007). Midbrain dopamine neurons are known to play an important role in establishing anticipatory neural activity in striatal and cortical brain regions in response to temporal regularity (Suri & Schultz, 2001). We therefore suggest that activation of the SN in the current study likely reflects the involvement of dopaminergic neurons in reinforcement-based temporal learning (Morris, Arkadir, Nevet, Vaadia, & Bergman, 2004).

Previous neuroimaging studies of CNV generation have mainly reported activations that were associated with the late wave in our paradigm. On the other hand, Nagai et al. (2004) also reported increased activity in motor regions, which were linked to iCNV in the current study. These results strongly suggest that short ISI paradigms present a superposition of early and late waves, with a predominance of the late component. Our results are at odds with the interpretation of Nagai et al., who proposed that ACC may be the origin of the early CNV component. A possible reason for this discrepancy, in addition to the use of a too short time interval to clearly discriminate iCNV and tCNV, may be their choice of a jittered ISI. Conceivably, uncertainty about the precise onset of the upcoming stimulus may affect the relative timings of early and late anticipation processes.

A potential shortcoming of the current study is that cortical potentials and fMRI were not acquired simultaneously, as has been elegantly achieved by Nagai et al. (2004). We were therefore unable to directly correlate electrophysiological and BOLD fMRI measures of neural activity. Simultaneous acquisition of EEG and fMRI in a CNV paradigm with long ISI would be equally desirable and challenging, mainly due to the difficulty of filtering MRI gradient artifacts from the slow cortical potentials (Laufs, Daunizeau, Carmichael, & Kleinschmidt, 2008).

Comparing Neural Processes of Response Conflict and Anticipation

A comparison of response conflict and anticipation processes in different tasks revealed shared brain regions underlying both processes, in line with a previous study (Fan et al., 2007) which compared conflict and expectancy in the same task. Importantly, however, the correspondence between both processes was only observed for late CNV components in the current study, whereas early anticipation implicated a different set of brain regions (see above).

Among the regions jointly activated during conflict and anticipation, a cluster in right FPC has been identified with conflict processing in a previous study from our lab (Lütcke & Frahm, 2008; COG distance less than 4 mm), as well as by several other groups (Zysset, Muller, Lohmann, & von Cramon, 2001; Carlson et al., 1998). Speculatively, FPC may be the source of top–down control which modulates task-specific regions such as the pre-SMA in the Flanker experiment or the thalamus during anticipation. In line with other authors (Corbetta & Shulman, 2002), we observed a right-hemispheric preference in this inferior frontal control system.

Overlapping activation in ACC, the anterior thalamus as well as anterior insular cortex suggests that both anticipatory behavior and conflict processing involve increased activity in the limbic system. Although traditionally seen as a neural substrate for emotions (Morgane, Galler, & Mokler, 2005), a number of components in the limbic system (including the aforementioned regions) are crucially involved in the regulation of autonomic functions (Critchley et al., 2003). Interestingly, both response anticipation and conflict have been linked to changes in autonomic arousal (Kobayashi, Yoshino, Takahashi, & Nomura, 2007; Freyschuss, Hjemdahl, Juhlin-Dannfelt, & Linde, 1988; Tecce, 1972). Common activation of a limbic network may therefore reflect modulation of autonomic function during conflict as well as anticipation, a hypothesis which awaits future confirmation by studies combining imaging and measurement of physiological parameters (see, e.g., Critchley, Tang, Glaser, Butterworth, & Dolan, 2005).

Within MFC, brain responses for anticipation and conflict overlapped largely in dorsal ACC, whereas differential activation was observed along the SFG (Figure 7A). Although conflict elicited stronger responses in a region corresponding to the pre-SMA, tCNV-related activations were observed in more anterior portions of the SFG. These results are in agreement with current conceptual models of MFC function. The pre-SMA, as the largest functional area along the SFG, is a task-specific region and is thought to mediate response selection by resolution of competing motor plans, such as the right- and left-hand responses in the Flanker paradigm (Nachev, Wydell, O'Neill, Husain, & Kennard, 2007; Sumner et al., 2007). Contrarily, dorsal ACC has been proposed to fulfill a more general role in the evaluation of stimulus saliency to guide adaptive behavior, in light of the organism's previous reward history (e.g., Rushworth, Buckley, Behrens, Walton, & Bannerman, 2007). In this context, ACC may recruit brain regions responsible for adjustment of autonomic arousal or allocation of top–down control. Speculatively, increased ACC activity at the end but not the beginning of the anticipation interval may reflect the cue's increasing salience for guiding the appropriate response toward the upcoming stimulus.

Together, the current results provide strong evidence for distinct brain regions subserving early and late components of response anticipation, as defined by their distinct neurophysiological signatures. We furthermore extend previous work and present evidence for a surprising similarity of activation patterns underlying response conflict and late, but not early, components of anticipatory behavior. Given the importance of expectancy and conflict resolution in the generation of

adaptive behavior, our results provide new insights into the neural architecture of fundamental aspects of human cognition.

Reprint requests should be sent to Henry Lütcke, Brain Research Institute, University of Zurich, Winterthurerstrasse 190, 8057 Zurich, Switzerland, or via e-mail: luetcke@hifo.uzh.ch.

REFERENCES

Aguirre, G. K., Zarahn, E., & D'Esposito, M. (1998). The variability of human, BOLD hemodynamic responses. *Neuroimage, 8,* 360–369.

Beckmann, C. F., Jenkinson, M., & Smith, S. M. (2003). General multilevel linear modeling for group analysis in FMRI. *Neuroimage, 20,* 1052–1063.

Beckmann, C. F., & Smith, S. M. (2004). Probabilistic independent component analysis for functional magnetic resonance imaging. *IEEE Transactions on Medical Imaging, 23,* 137–152.

Beckmann, C. F., & Smith, S. M. (2005). Tensorial extensions of independent component analysis for multisubject FMRI analysis. *Neuroimage, 25,* 294–311.

Bender, S., Resch, F., Weisbrod, M., & Oelkers-Ax, R. (2004). Specific task anticipation versus unspecific orienting reaction during early contingent negative variation. *Clinical Neurophysiology, 115,* 1836–1845.

Birbaumer, N., Elbert, T., Canavan, A. G., & Rockstroh, B. (1990). Slow potentials of the cerebral cortex and behavior. *Physiological Reviews, 70,* 1–41.

Carlson, S., Martinkauppi, S., Rama, P., Salli, E., Korvenoja, A., & Aronen, H. J. (1998). Distribution of cortical activation during visuospatial n-back tasks as revealed by functional magnetic resonance imaging. *Cerebral Cortex, 8,* 743–752.

Connor, W. H., & Lang, P. J. (1969). Cortical slow-wave and cardiac rate responses in stimulus orientation and reaction time conditions. *Journal of Experimental Psychology, 82,* 310–320.

Cools, R., Clark, L., & Robbins, T. W. (2004). Differential responses in human striatum and prefrontal cortex to changes in object and rule relevance. *Journal of Neuroscience, 24,* 1129–1135.

Corbetta, M., & Shulman, G. L. (2002). Control of goal-directed and stimulus-driven attention in the brain. *Nature Reviews Neuroscience, 3,* 201–215.

Critchley, H. D., Mathias, C. J., Josephs, O., O'Doherty, J., Zanini, S., Dewar, B. K., et al. (2003). Human cingulate cortex and autonomic control: Converging neuroimaging and clinical evidence. *Brain, 126,* 2139–2152.

Critchley, H. D., Tang, J., Glaser, D., Butterworth, B., & Dolan, R. J. (2005). Anterior cingulate activity during error and autonomic response. *Neuroimage, 27,* 885–895.

Eickhoff, S. B., Stephan, K. E., Mohlberg, H., Grefkes, C., Fink, G. R., Amunts, K., et al. (2005). A new SPM toolbox for combining probabilistic cytoarchitectonic maps and functional imaging data. *Neuroimage, 25,* 1325–1335.

Eriksen, B. A., & Eriksen, C. W. (1974). Effects of noise letters upon identification of a target letter in a nonsearch task. *Perception & Psychophysics, 16,* 143–149.

Fan, J., Kolster, R., Ghajar, J., Suh, M., Knight, R. T., Sarkar, R., et al. (2007). Response anticipation and response conflict: An event-related potential and functional magnetic resonance imaging study. *Journal of Neuroscience, 27,* 2272–2282.

Freyschuss, U., Hjemdahl, P., Juhlin-Dannfelt, A., & Linde, B. (1988). Cardiovascular and sympathoadrenal responses to mental stress: Influence of beta-blockade. *American Journal of Physiology, 255,* H1443–H1451.

Friedman, M. (1937). The use of ranks to avoid the assumption of normality implicit in the analysis of variance. *Journal of the American Statistical Association, 32,* 675–701.

Geyer, S., Ledberg, A., Schleicher, A., Kinomura, S., Schormann, T., Burgel, U., et al. (1996). Two different areas within the primary motor cortex of man. *Nature, 382,* 805–807.

Gomez, C. M., Marco, J., & Grau, C. (2003). Preparatory visuo-motor cortical network of the contingent negative variation estimated by current density. *Neuroimage, 20,* 216–224.

Gratton, G., Coles, M. G., & Donchin, E. (1983). A new method for off-line removal of ocular artifact. *Electroencephalography and Clinical Neurophysiology, 55,* 468–484.

Heinrich, H., Gevensleben, H., Freisleder, F. J., Moll, G. H., & Rothenberger, A. (2004). Training of slow cortical potentials in attention-deficit/hyperactivity disorder: Evidence for positive behavioral and neurophysiological effects. *Biological Psychiatry, 55,* 772–775.

Hyvärinen, A. (1999). Fast and robust fixed-point algorithms for independent component analysis. *IEEE Transactions on Neural Networks, 10,* 626–634.

Ikeda, A., Shibasaki, H., Kaji, R., Terada, K., Nagamine, T., Honda, M., et al. (1997). Dissociation between contingent negative variation (CNV) and Bereitschaftspotential (BP) in patients with parkinsonism. *Electroencephalography and Clinical Neurophysiology, 102,* 142–151.

Ioannides, A. A., Fenwick, P. B., Lumsden, J., Liu, M. J., Bamidis, P. D., Squires, K. C., et al. (1994). Activation sequence of discrete brain areas during cognitive processes: Results from magnetic field tomography. *Electroencephalography and Clinical Neurophysiology, 91,* 399–402.

Jenkinson, M., Bannister, P., Brady, M., & Smith, S. (2002). Improved optimization for the robust and accurate linear registration and motion correction of brain images. *Neuroimage, 17,* 825–841.

Kobayashi, N., Yoshino, A., Takahashi, Y., & Nomura, S. (2007). Autonomic arousal in cognitive conflict resolution. *Autonomic Neuroscience, 132,* 70–75.

Lancaster, J. L., Tordesillas-Gutierrez, D., Martinez, M., Salinas, F., Evans, A., Zilles, K., et al. (2007). Bias between MNI and Talairach coordinates analyzed using the ICBM-152 brain template. *Human Brain Mapping, 28,* 1194–1205.

Laufs, H., Daunizeau, J., Carmichael, D. W., & Kleinschmidt, A. (2008). Recent advances in recording electrophysiological data simultaneously with magnetic resonance imaging. *Neuroimage, 40,* 515–528.

Lewis, S. J., Dove, A., Robbins, T. W., Barker, R. A., & Owen, A. M. (2004). Striatal contributions to working memory: A functional magnetic resonance imaging study in humans. *European Journal of Neuroscience, 19,* 755–760.

Loveless, N. E., & Sanford, A. J. (1974). Effects of age on the contingent negative variation and preparatory set in a reaction-time task. *Journal of Gerontology, 29,* 52–63.

Lütcke, H., & Frahm, J. (2008). Lateralized anterior cingulate function during error processing and conflict monitoring as revealed by high-resolution fMRI. *Cerebral Cortex, 18,* 508–515.

Morgane, P. J., Galler, J. R., & Mokler, D. J. (2005). A review of systems and networks of the limbic forebrain/limbic midbrain. *Progress in Neurobiology, 75,* 143–160.

Morris, G., Arkadir, D., Nevet, A., Vaadia, E., & Bergman, H. (2004). Coincident but distinct messages of midbrain dopamine and striatal tonically active neurons. *Neuron, 43,* 133–143.

Nachev, P., Wydell, H., O'Neill, K., Husain, M., & Kennard, C. (2007). The role of the pre-supplementary motor area in the control of action. *Neuroimage, 36(Suppl. 2),* T155–T163.

Nagai, Y., Critchley, H. D., Featherstone, E., Fenwick, P. B., Trimble, M. R., & Dolan, R. J. (2004). Brain activity relating to the contingent negative variation: An fMRI investigation. *Neuroimage, 21,* 1232–1241.

Oikawa, H., Sasaki, M., Tamakawa, Y., Ehara, S., & Tohyama, K. (2002). The substantia nigra in Parkinson disease: Proton density-weighted spin-echo and fast short inversion time inversion-recovery MR findings. *AJNR, American Journal of Neuroradiology, 23,* 1747–1756.

Praamstra, P., Meyer, A. S., Cools, A. R., Horstink, M. W., & Stegeman, D. F. (1996). Movement preparation in Parkinson's disease. Time course and distribution of movement-related potentials in a movement precueing task. *Brain, 119,* 1689–1704.

Praamstra, P., & Pope, P. (2007). Slow brain potential and oscillatory EEG manifestations of impaired temporal preparation in Parkinson's disease. *Journal of Neurophysiology, 98,* 2848–2857.

Pulvermüller, F., Lutzenberger, W., Müller, V., Mohr, B., Dichgans, J., & Birbaumer, N. (1996). P3 and contingent negative variation in Parkinson's disease. *Electroencephalography and Clinical Neurophysiology, 98,* 456–467.

Rohrbaugh, J. W., Syndulko, K., & Lindsley, D. B. (1976). Brain wave components of the contingent negative variation in humans. *Science, 191,* 1055–1057.

Rushworth, M. F., Buckley, M. J., Behrens, T. E., Walton, M. E., & Bannerman, D. M. (2007). Functional organization of the medial frontal cortex. *Current Opinion in Neurobiology, 17,* 220–227.

Rushworth, M. F., Walton, M. E., Kennerley, S. W., & Bannerman, D. M. (2004). Action sets and decisions in the medial frontal cortex. *Trends in Cognitive Sciences, 8,* 410–417.

Smith, S. M. (2002). Fast robust automated brain extraction. *Human Brain Mapping, 17,* 143–155.

Sumner, P., Nachev, P., Morris, P., Peters, A. M., Jackson, S. R., Kennard, C., et al. (2007). Human medial frontal cortex mediates unconscious inhibition of voluntary action. *Neuron, 54,* 697–711.

Suri, R. E., & Schultz, W. (2001). Temporal difference model reproduces anticipatory neural activity. *Neural Computation, 13,* 841–862.

Taylor, S. F., Martis, B., Fitzgerald, K. D., Welsh, R. C., Abelson, J. L., Liberzon, I., et al. (2006). Medial frontal cortex activity and loss-related responses to errors. *Journal of Neuroscience, 26,* 4063–4070.

Tecce, J. J. (1972). Contingent negative variation (CNV) and psychological processes in man. *Psychological Bulletin, 77,* 73–108.

van Boxtel, G. J., & Brunia, C. H. (1994). Motor and non-motor aspects of slow brain potentials. *Biological Psychology, 38,* 37–51.

van Leeuwen, T. H., Steinhausen, H. C., Overtoom, C. C., Pascual-Marqui, R. D., van't Klooster, B., Rothenberger, A., et al. (1998). The continuous performance test revisited with neuroelectric mapping: Impaired orienting in children with attention deficits. *Behavioural Brain Research, 94,* 97–110.

Walter, W. G., Cooper, R., Aldridge, V. J., McCallum, W. C., & Winter, A. L. (1964). Contingent negative variation: An electric sign of sensorimotor association and expectancy in the human brain. *Nature, 203,* 380–384.

Wilcoxon, F. (1945). Individual comparisons by ranking methods. *Biometrics, 1,* 80–83.

Woolrich, M. W., Behrens, T. E. J., Beckmann, C. F., Jenkinson, M., & Smith, S. M. (2004). Multilevel linear modelling for FMRI group analysis using Bayesian inference. *Neuroimage, 21,* 1732–1747.

Woolrich, M. W., Ripley, B. D., Brady, M., & Smith, S. M. (2001). Temporal autocorrelation in univariate linear modeling of FMRI data. *Neuroimage, 14,* 1370–1386.

Worsley, K. J., Evans, A. C., Marrett, S., & Neelin, P. (1992). A three-dimensional statistical analysis for CBF activation studies in human brain. *Journal of Cerebral Blood Flow and Metabolism, 12,* 900–918.

Zysset, S., Muller, K., Lohmann, G., & von Cramon, D. Y. (2001). Color–word matching Stroop task: Separating interference and response conflict. *Neuroimage, 13,* 29–36.